Occurrence of nematic, topological, and Berry phases when a flat and a parabolic band touch

Balázs Dóra,[1,*] Igor F. Herbut,[2,3] and Roderich Moessner[3]

[1]*Department of Physics and BME-MTA Exotic Quantum Phases Research Group, Budapest University of Technology and Economics, Budafoki út 8, 1111 Budapest, Hungary*

[2]*Department of Physics, Simon Fraser University, Burnaby, British Columbia, Canada V5A 1S6*

[3]*Max-Planck-Institut für Physik komplexer Systeme, Nöthnitzer Strasse 38, 01187 Dresden, Germany*

(Received 10 March 2014; revised manuscript received 8 July 2014; published 24 July 2014)

A (single flavor) quadratic band crossing in two dimensions is known to have a generic instability towards a quantum anomalous Hall (QAH) ground state for infinitesimal repulsive interactions. Here we introduce a generalization of a quadratic band crossing which is protected only by rotational symmetry. By focusing on the representative case of a parabolic and flat band touching, which also allows for a straightforward lattice realization, the interaction induced nematic phase becomes the dominant instability in certain parts of the phase diagram already at weak coupling, by competing successfully with the QAH insulator. The full phase diagram of the model, together with its topological properties, is mapped out using a perturbative renormalization-group, strong-coupling analysis, the mean-field theory. Interestingly, the Berry flux varies continuously in the single flavor limit with various control parameters.

DOI: 10.1103/PhysRevB.90.045310 PACS number(s): 73.43.Nq, 71.10.−w, 05.30.Fk

I. INTRODUCTION

Topological states of matter possess the unique property that some of their response functions are universal, and independent of the sample-dependent microscopic parameters, such as scattering rate, interactions strength, etc. The early members of this family were the celebrated quantum Hall states, but with the advent of the topological insulator (TI) [1], numerous relatives have recently emerged. The topological protection of these materials mostly arises from their specific band structure, deriving from a strong spin-orbit interaction. Application-wise, TIs hold the promise to revolutionize spintronics, and to contribute to conventional and quantum computing.

It is interesting to contemplate different physical mechanisms that could lead to nontrivial topological properties. Several strategies other than band-structure engineering from the material science do exist. Time-periodic perturbations allow for modifying the Floquet band structure [2,3], this way influencing the topological properties of materials *in situ* without altering their composition. Applying strain to alter the band structure seems also feasible for a variety of materials [4].

The common theme in these ideas is nevertheless the direct modification of the single-particle band structure. Electron-electron interactions, however, can also produce the desired effect. Simple mean-field decoupling of the interaction can mimic an effective spin-orbit coupling, for example, thus inducing a transition from a topologically trivial to a nontrivial phase [5–8]. How precisely this happens, and how competitive the topologically nontrivial phases in general are, is an open question which often calls for more elaborate analysis [9]. The uncertainties notwithstanding, clear-cut answers are available for two-dimensional systems with Fermi points instead of the usual Fermi surface. In Refs. [10,11], for example, it was argued that a single quadratic band crossing, protected by time reversal and rotational symmetry, is unstable with respect to topological insulating phases.

Here we formulate a more general quadratic band crossing Hamiltonian in two dimensions, protected only by rotational symmetry. A single copy of such a band crossing contains all three Pauli matrices and thus naturally breaks time-reversal symmetry (TRS) and possesses a nontrivial Berry phase. We focus on the representative case of a flat and parabolic band touching, although our results apply more generally (see below). We show that the nematic order becomes the dominant instability within a certain range of the parameters for weak couplings. This happens even though the broken TRS might most naturally have suggested a quantum anomalous Hall (QAH) type phase, which indeed does dominate in related models [10,11]. In particular, our (continuum) model features a metastable phase purely nematically ordered, and without the QAH effect, in contrast to the standard result [10]. We also propose a simple lattice realization of our generalized quadratic band crossing Hamiltonian which could serve as an atomic physics platform for the experimental study of the competition between the different interaction-induced phases considered here.

II. MODEL AND BASIC PROPERTIES

Our generalization of the two-dimensional quadratic band crossing Hamiltonian [10] has a rotationally invariant spectrum, featuring however all *three* Pauli matrices,

$$H_0 = -\frac{p^2}{4m'}\mathbb{I} - \frac{p^2 c}{4m}\sigma_3 - \frac{s}{4m}\left[\sigma_1\left(p_x^2 - p_y^2\right) + \sigma_2 2p_x p_y\right], \tag{1}$$

with the parameters $c = \cos(2\alpha)$, $s = \sin(2\alpha)$. Although its spectrum is independent of α, the topological properties are not. Equation (1) exhibits a quadratic band crossing with generally unequal effective masses for $|m| \leqslant |m'|$ [12]. We focus on the representative case with $m = m'$, when one of the bands becomes flat, but all of our results apply to the more general situation.

*dora@eik.bme.hu

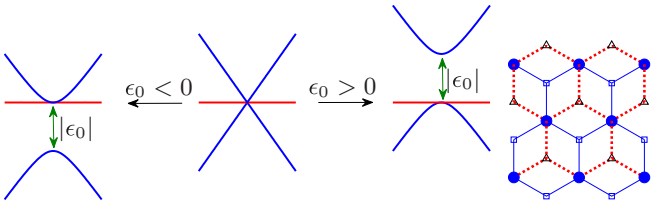

FIG. 1. (Color online) Left: The evolution of the noninteracting spectrum with ϵ_0 is shown together with the resulting quadratic and flat band touching. The horizontal red line denotes the flat band, which remains fixed. Right: the dice lattice with $t\cos(\alpha)$ and $t\sin(\alpha)$ hopping along the blue solid and red dashed lines. The on-site energy of the sixfold connected filled blue sites, which are integrated out, is ϵ_0.

For $c = 0$ ($\alpha = \pi/4$), this reduces to the model studied in Ref. [10]. Due to the presence of all three Pauli matrices, the Hamiltonian necessarily violates the TRS. The spectrum consists of two bands, one completely flat and another dispersive $\sim -p^2/2m$ (see Fig. 1). For $m > 0$, the low-energy dynamics is described by a filled inverted parabolic band touching an empty flat band at its maximum. For $m < 0$, a filled flat band touches an empty parabolic band at its minimum. In spite of the explicit dependence of the Hamiltonian on α, its spectrum of eigenvalues is independent from it. The eigenvectors, on the other hand, do depend on α, as $|0\rangle_p = [\sin(\alpha), -\cos(\alpha)\exp(2i\varphi_p)]^T$ and $|p^2\rangle_p = [\cos(\alpha), \sin(\alpha)\exp(2i\varphi_p)]^T$. In both cases, the flat band touches the parabolic band at a single point in momentum space, producing a Berry phase of $2\pi(1 \pm c)$ for the flat and parabolic bands, respectively, that depends continuously on α. These non-π-quantized Berry phases indicate a no-go theorem for the Hamiltonian H_0, and require an even number of band touchings as described by Eq. (1), similarly to the Dirac equation in graphene. The exception is when $c = 0$ or $s = 0$, when some of the three Pauli matrices are absent, as in Refs. [10,13–15]. In what follows we will focus on the case $m < 0$, but our results can directly be translated to the case $m > 0$ as well.

Equation (1) remains invariant upon shifting α by π, and the ground-state properties of the system are even functions of α, since its sign change can be compensated by a $\pi/2$ rotation of the momentum. It suffices therefore to focus on α in the interval $[0,\pi/2]$. The "sublattice" symmetry is naturally broken in Eq. (1), unless $\alpha = \pi/4$, since $\langle\Psi_1^+\Psi_1\rangle_0 = \rho_0 W\sin^2(\alpha)$ and $\langle\Psi_2^+\Psi_2\rangle_0 = \rho_0 W\cos^2(\alpha)$ in the noninteracting ground state. Here, $\Psi_{1,2}$ are the field operators for the two species of electrons, W is the high-energy cutoff, and $\rho_0 = |m|/2\pi$ is the constant density of states in the parabolic band. The system is thus naturally a "charge density wave" when $\alpha \neq \pi/4$.

Quadratic Hamiltonians resembling ours, but lacking the third Pauli matrix, arise in an effective collinear spin-density-wave theory [16], from the surface states of certain Weyl semimetals [17], as well as from the Lieb lattice [18].

Next, we define the full (interacting) low-energy Hamiltonian:

$$H = \int d\mathbf{r}[\mathbf{\Psi}^+(\mathbf{r})H\mathbf{\Psi}(\mathbf{r}) + U\delta n_1(\mathbf{r})\delta n_2(\mathbf{r})], \qquad (2)$$

where the spinor $\mathbf{\Psi}^+ = (\Psi_1^+, \Psi_2^+)$, U is the strength of the coupling constant, and $\delta n_l = \Psi_l^+\Psi_l - \langle\Psi_l^+\Psi_l\rangle_0$, with $l = 1$, 2, stands for the densities measured from their noninteracting values. The second term can be regarded as a fine-tuning of the interaction, which can be provided by single-particle terms of the form, e.g., $\Psi_1^+\Psi_1\langle\Psi_2^+\Psi_2\rangle_0$. Without this careful subtraction of the noninteracting densities a constant self-energy $\propto U\sigma_3$ would be generated, gapping out the spectrum already at the Hartree level. This effect occurs for the semi-Dirac points [19], and here comes as a consequence of the broken sublattice symmetry at a general $\alpha \neq \pi/4$ mentioned earlier.

III. LATTICE REALIZATION

Equation (1) can describe a modified dice or T_3 lattice, consisting of three layers of triangular lattices with only intersublattice hoppings between adjacent layers, or two honeycomb lattices sharing one sublattice, shown in Fig. 1. The Hamiltonian matrix reads [20–22]

$$H_{\text{dice}} = \begin{pmatrix} 0 & t_1 f_{\mathbf{k}} & 0 \\ t_1 f_{\mathbf{k}}^* & \epsilon_0 & t_2 f_{\mathbf{k}} \\ 0 & t_2 f_{\mathbf{k}}^* & 0 \end{pmatrix}, \qquad (3)$$

where t_1 and t_2 are the hopping integrals between adjacent triangular lattices, ϵ_0 is an on-site potential in the middle layer (arising from, e.g., a real chemical potential, or from the Hartree term of a short-range interaction) and $f_{\mathbf{k}} = 1 + 2\exp(i3k_y/2)\cos(\sqrt{3}k_x/2)$. If ϵ_0 is large compared to the energies of interest, the electrons on the middle layer can be integrated out [14] yielding the effective two-band Hamiltonian

$$H_{\text{dice}}^{\text{eff}} = -\frac{1}{\epsilon_0}\begin{pmatrix} |t_1 f_{\mathbf{k}}|^2 & t_1 t_2 f_{\mathbf{k}}^2 \\ t_1 t_2 f_{\mathbf{k}}^{*2} & |t_2 f_{\mathbf{k}}|^2 \end{pmatrix}. \qquad (4)$$

One set of the eigenvalues of the effective Hamiltonian is a completely dispersionless flat band, whereas the other one reads as $-(t_1^2 + t_2^2)|f(\mathbf{k})|^2/\epsilon_0$. Around the K point in the Brillouin zone one can linearize the function $f(\mathbf{K} + \mathbf{p}) \approx (3/2)(p_x - ip_y)$, and upon further parametrizing the hopping integrals in terms of an "angle" α as $t_1 = t\cos(\alpha)$, $t_2 = t\sin(\alpha)$, the low-energy dynamics is described by Eq. (1) with $m = 2\epsilon_0/9t^2$, $t = \sqrt{t_1^2 + t_2^2}$. Similarly as in graphene, a time-reversed copy of the Hamiltonian with $\sigma_2 \to -\sigma_2$ describes the low-energy physics at the opposite corner of the hexagonal Brillouin zone, at the point K'. The two Hamiltonians at the K and K' points map onto each other under time reversal, and therefore taken together preserve the TRS. Nevertheless, for the sake of simplicity, in studying the effects of interactions our focus will mainly be on a single valley.

IV. WEAK-COUPLING ANALYSIS

The model at hand shares similarities with those for bilayer graphene [11,13,23,24] and the simpler quadratic band touching in two dimensions [10]. The dynamic critical exponent is $z = 2$, which together with the spatial dimensionality of 2 predicts short-range interactions to be precisely marginal at the tree level. By performing the standard one-loop renormalization group (RG), assuming the flat band to be

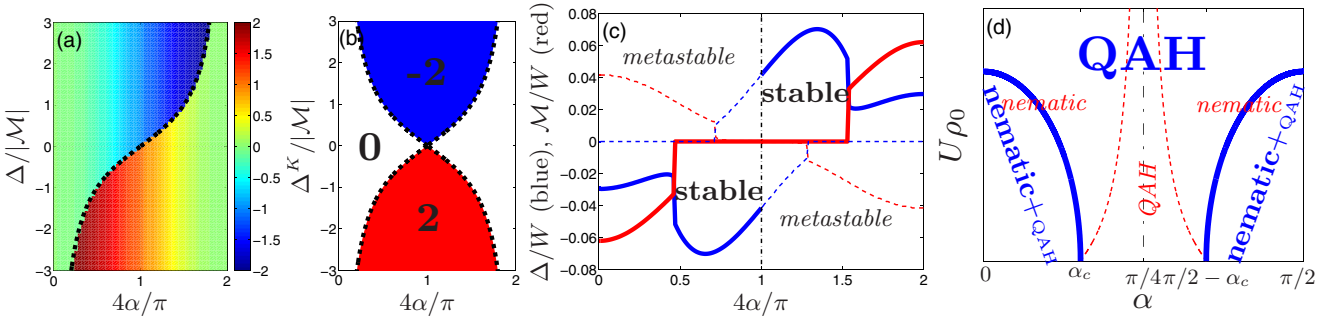

FIG. 2. (Color online) (a) the Berry flux for the single valley Hamiltonian in Eq. (1) with QAH and nematic order parameters, becoming quantized only when c or s vanishes. The Berry flux jumps when $\Delta/|\mathcal{M}| = -c/|s|$. (b) the Chern number of two time-reversed copies of Eq. (1) at the K and K' points with $\Delta^K = -\Delta^{K'}$ (relevant for the dice lattice). The phase boundaries between phases with different Chern numbers are given by $\Delta^K/|\mathcal{M}| = \pm c/s$. For $\Delta^K = \Delta^{K'}$, the Chern number is identically zero. The phase of the nematic order parameter has no effect on the two left panels. (c) the typical evolution of the order parameters is shown for $U\rho_0 = 0.31$. The sign of the QAH order is well defined (i.e., its sign change would alter the ground-state energy) since it is reached through a first-order phase transition for $\alpha \neq \pi/4$. At $\alpha = \pi/4$, the transition is second order and is identical to Ref. [10]. (d) Schematic phase diagram in the U-α plane. The stable solutions are depicted in blue, while the metastable part is in red. The transition is first order across the lines between the various phases on either side of the black dash-dotted line, along which the transition is second order to a QAH state.

fully filled and the parabolic band to be empty, the repulsive interactions turn out to be marginally *relevant*. In fact, exactly as in the previously studied case of a single-valley quadratic band crossing [10], the particle-particle diagram vanishes and only the particle-hole diagrams contribute. This can be understood as a consequence of the absence of the "fermionic" (negative when squared) time-reversal symmetry necessary for Cooper pairing [25] in both cases. The resulting β function is then

$$\frac{dU}{d\ln s} = U^2\rho_0 + O(U^3), \tag{5}$$

which is, unexpectedly, completely independent of the parameter α, at least to the leading order. Here we integrated out the fermions with momenta within the shell $[W/s, W]$ and with all Matsubara frequencies. To the leading order in U neither the angle α nor the mass in Eq. (1) flow.

In order to determine the type of ordering that ensues, we rewrite the interaction in a more suggestive form as

$$8\Psi_1^+\Psi_1\Psi_2^+\Psi_2 = (\mathbf{\Psi}^+\mathbf{\Psi})^2 - \sum_{l=1}^{3}(\mathbf{\Psi}^+\sigma_l\mathbf{\Psi})^2, \tag{6}$$

from which the orderings preferred by the repulsive interaction are identified as

$$\Delta = -\frac{U}{2}(\langle\mathbf{\Psi}^+\sigma_3\mathbf{\Psi}\rangle - \langle\mathbf{\Psi}^+\sigma_3\mathbf{\Psi}\rangle_0), \tag{7a}$$

$$\mathcal{M}\exp(i\theta) = -\frac{U}{2}\langle\mathbf{\Psi}^+(\sigma_1 + i\sigma_2)\mathbf{\Psi}\rangle, \tag{7b}$$

where θ keeps track of the relative phase of the two nematic order parameters. All of these yield a fully gapped spectrum for $\alpha \neq \pi/4$, and since Eq. (1) contains all three Pauli matrices, they also feature a finite zero-field Hall conductivity, which is, however, not quantized in general. This parallels closely the noninteger quantized Hall response of a single Dirac cone [26], which only gets quantized upon considering its time-reversal partner, similarly to graphene. The Δ corresponds to the QAH state, which gaps out the spectrum and does not break any additional symmetry, such as time reversal, when $\alpha \neq \pi/4$, since all three Pauli matrices are already present in the bare Hamiltonian in Eq. (1). Only when $\alpha = \pi/4$ and the matrix σ_3 is absent does the QAH phase break the TRS. On the other hand, $\mathcal{M}$ describes the nematic orderings, which would result from the spontaneous reduction of the C_6 rotational symmetry down to C_2, with the full rotational symmetry of the spectrum broken [see Eq. (9)]. When $c = 0$, the nematic phase becomes gapless with two linearly dispersing Dirac cones, similarly to Refs. [10,11], and its zero-field Hall conductivity vanishes. The Berry flux [1,22], i.e., the integral of the Berry curvature around a single valley, is shown in Fig. 2 in the presence of QAH and nematic orderins. The Berry flux is nonzero even in the nematic phase due to the broken TRS in H_0. Surprisingly, it varies continuously similarly to the Berry phase and can take any value between -2 and 2, which is not expected from a topological invariant. It becomes quantized when even copies of Eq. (1) are considered, signaling a no-go theorem for H_0.

The ratio of the susceptibilities corresponding to these order parameters is α dependent:

$$\frac{\chi_\Delta}{\chi_\mathcal{M}} = \frac{2s^2}{2-s^2}. \tag{8}$$

Although the spectrum, and even the RG flow of the interaction, were oblivious to the parameter α, it nevertheless determines the leading susceptibility, and thus the ultimate nature of the instability at weak coupling. The nematic and QAH susceptibilities are equal only at a critical value α_c, given by $\sin^2(2\alpha_c) = 2/3$. The QAH state is realized when $|\sin(2\alpha)| > \sqrt{2/3}$, with the nematic order being otherwise dominant.

In the case of two valleys, relevant to the dice lattice, the order parameter Δ with different signs in the two valleys breaks TRS and results in an overall finite QAH effect. On the dice lattice, this could be realized by intrasublattice, non-on-site interactions à la extended Hubbard model which can be decoupled to favor the QAH order, as was done on the honeycomb lattice [5,6]. In the case of identical signs, Δ only

additionally contributes to the amplitude of the charge density wave, which already exists for general $\alpha \neq \pi/4$. Albeit the nematic order parameter possesses a nonzero Berry flux in a single valley, the contribution from the other valley with opposite chirality always compensates it to zero, at least in the physically motivated case when the absolute value of the the two order parameters in the two valleys are equal. When QAH and nematic order coexist, the Chern numbers are shown in Fig. 2.

V. STRONG-COUPLING ANALYSIS

Without the kinetic-energy term ($t = 0$), the interaction clearly favors deviations from the particle densities in the noninteracting limit, with either $\langle \delta n_1 \rangle > 0$ and $\langle \delta n_2 \rangle < 0$, or vice versa. Depending on the particle densities in the noninteracting limit, one of these would be energetically favorable, and the ground-state energy profile as a function of the respective particle densities develops an asymmetric double-well structure, leading to a first-order transition. At $\alpha = \pi/4$, the depths of the two wells become equal, and the order of the transition changes from first to second. As a result, the system will be a "fully polarized" charge density wave in the sense that one sublattice is fully occupied while the other is empty. This corresponds to $\Delta \neq 0$, i.e., the analog of the QAH state for all values of α.

Connecting the weak- and strong-coupling regimes when $|\sin(2\alpha)| < \sqrt{2/3}$ requires therefore a quantum phase transition from the nematic to the QAH state with increasing interaction. The details of this transition are evidently beyond the reach of the weak-coupling RG calculations, and so we formulate a mean-field theory in order to study it further. For $|\sin(2\alpha)| > \sqrt{2/3}$, on the other hand, the same QAH state appears at both strong and weak couplings.

VI. MEAN-FIELD THEORY

Allowing for all three kinds of orderings, the mean-field decoupling of the interaction gives the energy spectrum

$$E_{\pm}(\mathbf{p}) = \frac{\varepsilon_p}{2} \pm \sqrt{\frac{\varepsilon_p^2}{4} + \varepsilon_p[\mathcal{M}s\cos(2\varphi_p - \theta) + \Delta c] + \Delta^2 + \mathcal{M}^2}, \tag{9}$$

where $\varepsilon_p = p^2/2|m|$.

The ground-state energy per unit cell is

$$E = \frac{\Delta^2 + \mathcal{M}^2}{U} + \int \frac{d^2p}{(2\pi)^2} E_-(\mathbf{p}) + W\rho_0 \Delta c, \tag{10}$$

subject to minimization with respect to Δ and $\mathcal{M}$. The last term arises from the fine tuning of the interaction in terms of the noninteracting densities. The relative angle of the nematic order parameters θ drops out from the calculation. Were the rotational symmetry of the spectrum already broken in Eq. (1) by, for example, choosing unequal prefactors of the σ_1 or σ_2 term, the preferred value of θ would also be determined by the mean-field equations, and the competition between different nematic orders and the QAH phase would be more subtle.

The Ginzburg-Landau expansion of E contains even and odd powers of Δ, therefore the energy landscape exhibits an asymmetric double well structure, leading to a first-order phase transition. On the other hand, only even powers of $\mathcal{M}$ are present in E, yielding a second-order phase transition for the nematic order. Close to $\alpha \lesssim \pi/4$, a pure QAH state is stable for $U\rho_0 \ll 1$, and

$$\Delta = \frac{W}{c-1} \exp\left(-\frac{1}{U\rho_0 s^2} + \frac{c}{1-c} \right), \tag{11}$$

displaying the characteristic essential singularity in the weak-coupling limit. For $\alpha \gtrsim \pi/4$, Eq. (11) describes a metastable solution, with the stable solution obtained from it by the replacement $\alpha \to \pi/2 - \alpha$, and change in sign of the right-hand side of Eq. (11). This is depicted in Fig. 2. The nematic order dominates around $\alpha \sim 0$ with a similar interaction dependence $\ln(W/\mathcal{M}) \sim 1/U\rho_0$, but with a more complicated full expression. These two orders possess the same ground-state energy for $\sin^2(2\alpha) = 2/3$, as predicted by the susceptibilities. However, the nematic order parameter always coexists with a secondary, parasitic QAH order for the stable solution, satisfying $\Delta \sim U\rho_0 \mathcal{M}$ in the extreme weak coupling, $U\rho_0 \ll 1$ limit. With increasing interaction, this coexistence region shrinks and the region with pure QAH as the primary order parameter gains in territory.

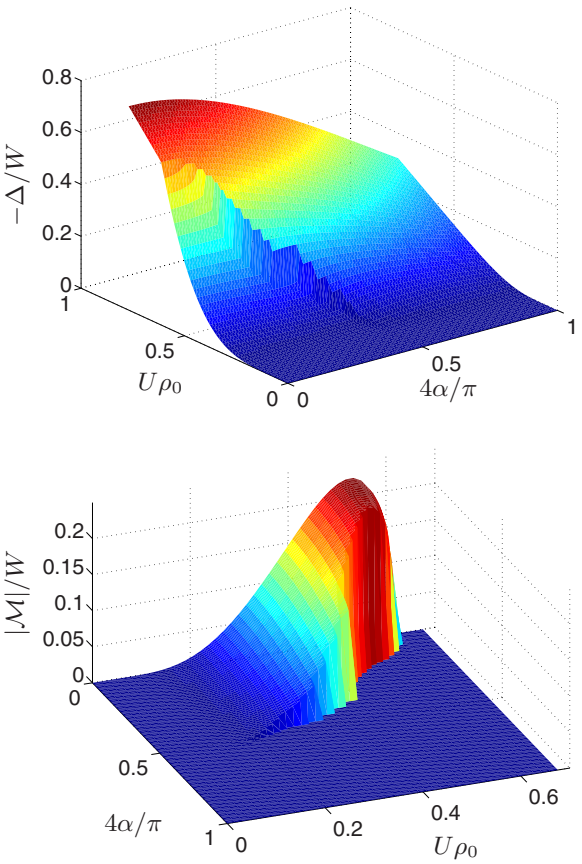

FIG. 3. (Color online) The interaction and α dependence of the stable order parameters is shown.

A typical evolution of ordering with α is depicted in Fig. 2 in the weak-coupling limit. The QAH and nematic phases coexist only for the stable solution, and exclude each other in the metastable solutions of the first-order transition. The $\Delta = \mathcal{M} = 0$ case always represents an unstable solution to the gap equations. The full phase diagram, visualizing both stable and metastable regions, is plotted schematically in Fig. 2, constructed from the numerical solution of the gap equations. As predicted by the RG, there is a wide region for a QAH and nematic (accompanied by a subdominant QAH) phases. With increasing U, the region of the nematic state shrinks, and eventually for large U through a quantum phase transition gives way to the pure QAH state, in accordance with the considerations at strong coupling. The numerical solution of the gap equations, minimizing E, is shown in Fig. 3 for the stable solutions.

VII. EXPERIMENTAL REALIZATIONS

The dice lattice with unequal hoppings and distinct sublattice potentials can be realized experimentally in a controlled way with cold atoms loaded in an optical lattice [22,27]. The interaction strength is tunable by, e.g., a Feshbach resonance and by tuning the parameter α, so that our predictions can directly be tested. In condensed matter, the dice lattice arises from a trilayer structure of the face-centered-cubic lattice, grown in the [111] direction [22], with $SrTiO_3/SrIrO_3/SrTiO_3$ trilayer heterostructures [28] promising in this respect. Finally, the dice lattice can also be created by generalizing artificial graphene's honeycomb lattice [29].

Cold atomic settings, unlike solid-state ones, can host metastable states with a long lifetime due to the excellent control over various relaxation channels, offering the possibility to explore the full phase diagram. Since both nematic and QAH states are gapped, a near-adiabatic tuning of α allows for passing through the stable to the metastable region. Moreover, when two copies of our low-energy Hamiltonian, one for each valley, are realized by a given lattice model, a stable QAH state in one valley and a metastable one in the other valley would always realize a metastable topological insulating phase.

VIII. CONCLUSION

We have investigated a generalized quadratic band crossing with only rotational symmetry and broken TRS. Surprisingly, a single valley Hamiltonian favors nematic ordering as the dominant instability in certain parameter range, though the broken TRS would have suggested the QAH effect (in the same way as, e.g., a finite magnetic field induces a finite magnetization). In particular, although the RG equation for the interaction is the same as in Ref. [10], the QAH and nematic susceptibilities depend strongly on α. Moreover, with increasing interaction, the nematic order disappears and QAH ordering dominates.

ACKNOWLEDGMENTS

Illuminating discussions with E. Szirmai on the RG are gratefully acknowledged. B.D. was supported by the Hungarian Scientific Research Fund Nos. K101244, K105149, K108676, CNK80991, ERC Grant No. ERC-259374-Sylo, and by the Bolyai Program of the HAS. I.F.H. was supported by the NSERC of Canada.

[1] M. Z. Hasan and C. L. Kane, Rev. Mod. Phys. **82**, 3045 (2010).
[2] N. H. Lindner, G. Refael, and V. Galitski, Nat. Phys. **7**, 490 (2011).
[3] J. Cayssol, B. Dóra, F. Simon, and R. Moessner, Phys. Status Solidi RRL **7**, 101 (2013).
[4] F. Guinea, Solid State Commun. **152**, 1437 (2012).
[5] S. Raghu, X.-L. Qi, C. Honerkamp, and S.-C. Zhang, Phys. Rev. Lett. **100**, 156401 (2008).
[6] E. V. Castro, A. G. Grushin, B. Valenzuela, M. A. H. Vozmediano, A. Cortijo, and F. de Juan, Phys. Rev. Lett. **107**, 106402 (2011).
[7] I. F. Herbut, Phys. Rev. B **78**, 205433 (2008).
[8] B. Roy and I. F. Herbut, Phys. Rev. B **88**, 045425 (2013).
[9] T. Đurić, N. Chancellor, and I. F. Herbut, Phys. Rev. B **89**, 165123 (2014).
[10] K. Sun, H. Yao, E. Fradkin, and S. A. Kivelson, Phys. Rev. Lett. **103**, 046811 (2009).
[11] O. Vafek and K. Yang, Phys. Rev. B **81**, 041401 (2010).
[12] Note that $|m| > |m'|$ implies the touching of two inverted or normal parabola.
[13] R. Nandkishore and L. Levitov, Phys. Rev. B **82**, 115124 (2010).
[14] O. Vafek, Phys. Rev. B **82**, 205106 (2010).
[15] Y. You and E. Fradkin, Phys. Rev. B **88**, 235124 (2013).
[16] G.-W. Chern and C. D. Batista, Phys. Rev. Lett. **109**, 156801 (2012).
[17] G. Xu, H. Weng, Z. Wang, X. Dai, and Z. Fang, Phys. Rev. Lett. **107**, 186806 (2011).
[18] W.-F. Tsai, C. Fang, H. Yao, and JiangPing Hu, arXiv:1112.5789.
[19] B. Dóra, I. F. Herbut, and R. Moessner, Phys. Rev. B **88**, 075126 (2013).
[20] J. Vidal, R. Mosseri, and B. Douçot, Phys. Rev. Lett. **81**, 5888 (1998).
[21] D. Bercioux, D. F. Urban, H. Grabert, and W. Hausler, Phys. Rev. A **80**, 063603 (2009).
[22] B. Dóra, J. Kailasvuori, and R. Moessner, Phys. Rev. B **84**, 195422 (2011).
[23] F. Zhang, H. Min, M. Polini, and A. H. MacDonald, Phys. Rev. B **81**, 041402 (2010).
[24] Y. Lemonik, I. L. Aleiner, Cs. Tőke, and V. I. Fal'ko, Phys. Rev. B **82**, 201408 (2010).
[25] I. F. Herbut, Phys. Rev. D **87**, 085002 (2013).
[26] A. W. W. Ludwig, M. P. A. Fisher, R. Shankar, and G. Grinstein, Phys. Rev. B **50**, 7526 (1994).
[27] A. Raoux, M. Morigi, J.-N. Fuchs, F. Piéchon, and G. Montambaux, Phys. Rev. Lett. **112**, 026402 (2014).
[28] F. Wang and Y. Ran, Phys. Rev. B **84**, 241103 (2011).
[29] K. K. Gomes, W. Mar, W. Ko, F. Guinea, and H. C. Manoharan, Nature (London) **483**, 306 (2012).